

the particle path is a screw helix viewed off-axis, D is an underestimate of the true diameter; a closer measure of the true diameter is D' (Fig. 1). Since for $D/D' < 1$ we underestimate the diameter and the period, it is necessary to apply a correction calculated to be 10% to the circulation ($\propto D^2/t$) when $D/D' = 0.8$. This correction, made on data shown in Fig. 2(b), 2(c), and 2(d), is required for about one point in five. In all cases, D and t were measured, and a correction, if necessary, decided upon before n was calculated after which, to avoid bias, no re-evaluation was permitted.

⁸The number of events in Fig. 2(d) at $n=1$ (not 0.8), 2, 3, 4, and 5 were analyzed with Pearson's χ^2 test. Compared to several smooth analytical curves adjusted to have an area equal to the histogram, the probability of the observed positive deviations being random fluctuations was less than 0.02.

⁹D. Y. Chung and P. R. Critchlow, Phys. Rev. Letters **14**, 892 (1965) find that H-D particles in a superfluid wind tunnel do not remain at rest as the normal fluid presumably is, but are dragged by the superfluid for $v_s > 1.4$ mm/sec. In the counterflow experiments of reference 4, particles move at less than the normal fluid velocity (v_n) for $v_n > 1$ mm/sec ($v_s > 0.1$ mm/sec at low temperatures). This velocity retardation is presumably due to interactions with the counterflowing superfluid component.

¹⁰One might consider that the $n=2, 3$, etc. points in Fig. 2 are associated with orbits around several $n=1$ lines of the same polarity. However, in the rotation system there are only 10 to 30 lines/mm², yet many "circles" 0.07 to 0.1 mm in diameter have n 's of about 2 and 3 [Figs. 1 and 2(c)]. This is improbable, unless there is a clumping of lines—a higher energy, unstable arrangement.

THERMAL EXPANSION COEFFICIENT AND COMPRESSIBILITY OF SOLID He³†

E. D. Adams, G. C. Straty, and E. L. Wall*

Physics Department, University of Florida, Gainesville, Florida
(Received 16 August 1965)

Liquid helium has been the object of extensive research for many years, while considerably less attention has been devoted to solid helium. Particularly lacking have been direct measurements of the thermal expansion coefficient and compressibility of solid helium, although theoretical calculations¹⁻³ and calculations from other data^{4,5} have been made. This lack of experimental data is due to the difficulty of measuring accurately the small changes in pressure resulting from changes in temperature of the solid. We report here direct observations of the thermal expansion coefficient and compressibility of solid He³. The measurements are all in the bcc phase for molar volumes from 22.39 to 24.61 cm³/mole and over the temperature range from 0.3°K to the melting point.

A capacitance-type strain gauge which permitted observation of changes in pressure on the solid sample of less than 10⁻³ atm was used. The details of the sample chamber and pressure measuring apparatus will be reported elsewhere.⁶

For each sample studied the solid was obtained by applying pressure at a temperature just above the melting point. The filling capillary above the sample chamber was then blocked by quickly cooling it below the melting point, usually to 0.3°K, where it was held

during the course of the measurements on a given sample. Observations of pressure versus temperature, made for both decreasing and increasing temperature with up to several hours time lapse between, showed good reproducibility. This indicated that there was negligible slipping of the solid blocking the capillary and very little hysteresis in the strain gauge. For a change in temperature from 0.3°K to the melting temperature the fractional change in pressure was of the order of 1%, while the fractional change in volume due to stretching of the sample chamber was calculated to be of the order of 0.001%. Therefore, for all practical purposes, the process was at constant volume.

To obtain the compressibility, $P(T)$ was measured for various molar volumes. The molar volume for each sample was determined from the intersection of the isochore with the melting curve using the data of Mills, Grilly, and Sydoriak.⁴ A plot of V vs P for fixed temperatures was then made, with the slope of these curves determining the compressibility $\beta = -V^{-1}(\partial V/\partial P)_T$. The values of β obtained in this way are shown in Fig. 1. Because of the extremely small temperature dependence of β , only the values at 0.3°K are shown. Data from other sources are shown for comparison. Our results compare reasonably well with those

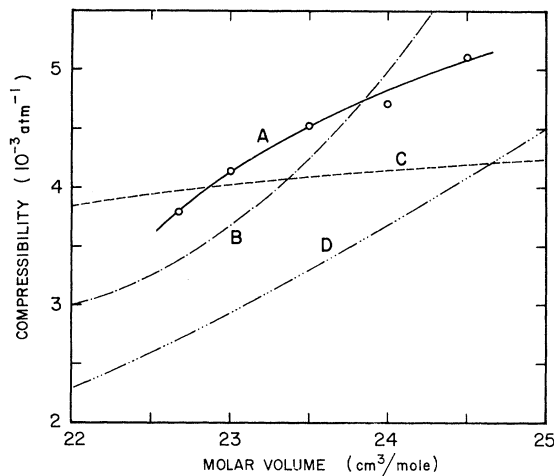


FIG. 1. The compressibility of He³ versus molar volume. Curve A, this work at 0.3°K; curve B, values at the melting temperature computed from specific heat data by Heltemes and Swenson⁵; curve C, theoretical calculation of Saunders¹; curve D, liquid at the melting temperature.

of Heltemes and Swenson⁵ computed from specific heat data. As was pointed out by Heltemes and Swenson, we have here the unusual situation of the compressibility of the solid being greater than that of the liquid.

With β determined, the thermal expansion coefficient $\alpha = V^{-1}(\partial V/\partial T)_P = \beta(\partial P/\partial T)_V$ was found from the slopes of the isochores. A slight error is introduced since the $P(T)$ curves are not at strictly constant volumes. The following considerations show that this is negligible. For a process in which P , V , and T all change, α and β are related by

$$\alpha = \left(\beta + \frac{1}{V} \frac{dV}{dP} \right) \frac{dP}{dT}. \quad (1)$$

If $dV=0$ this reduces to $\alpha = \beta(\partial P/\partial T)_V$. While β is of the order of 10^{-3} atm^{-1} , $V^{-1}dV/dP$ is determined by properties of the sample chamber and, in this experiment, was of the order of 10^{-5} atm^{-1} . Thus an error of about 1% is introduced in assuming $dV=0$.

Figure 2 shows values of the expansion coefficient plotted versus temperature for various molar volumes. The vertical bar near the end of each curve is the melting temperature for that particular molar volume. The expansion coefficients at the melting temperature are difficult to determine since the slopes of the isochores are changing rapidly. Also the extrapolation of the α vs T curves to the melt-

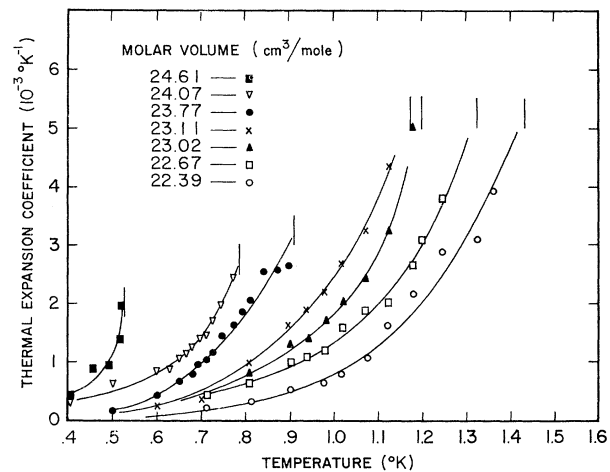


FIG. 2. The thermal expansion coefficient of solid He³ versus temperature for various molar volumes. The vertical bar near the end of each curve indicates the melting temperature.

ing temperature is somewhat uncertain, especially for the curves at molar volumes of 23.02 and 23.11 cm³/mole. It should be pointed out that no negative expansion coefficients have been observed, in contrast to theoretical predictions^{2,3} and calculations from other data.⁴ Thus the supposed anomalous behavior has not been observed. The calculations of reference 4 were based on the reasonable, but incorrect, assumption that $\beta_{\text{liquid}} > \beta_{\text{solid}}$ along the melting curve.

Although α and β are independent quantities, they can be checked for consistency along the melting curve. Applying Eq. (1) at the melting curve, we have

$$\alpha_m = \beta_m \left(\frac{dP}{dT} \right)_m + \frac{1}{V} \left(\frac{dV}{dT} \right)_m. \quad (2)$$

If either α_m or β_m is given the other can be calculated. Because the two terms on the right are of almost equal magnitude but of opposite sign, calculated values of β_m are very insensitive to changes in α_m . If α_m is calculated using the measured values of β_m , the opposite is true, and only qualitative comparison between the calculated values and measured values can be made. The calculated α_m , using the measured β_m and the data of Mills, Grilly, and Sydoriak⁴ for evaluating the other factors in Eq. (2), are shown in the following table:

T_m (°K)	0.6	0.8	1.0	1.2	1.4
Calculated α_m (10^{-3} atm^{-1})	~0	5	7	17	10

Referring to Fig. 2, we see that these values are roughly twice those obtained from extrapolation to T_m . Considering the previously mentioned uncertainties in the calculated values of α_m and in the extrapolation of the measured α to the melting temperature, the qualitative comparison is good.

We would like to acknowledge the assistance of M. F. Panczyk and R. A. Scribner in taking some of the data.

†Research supported by the National Science Foundation.

*Present address: Cryonetics, Inc., Burlington, Massachusetts.

¹E. M. Saunders, Phys. Rev. **126**, 1724 (1962).

²N. Bernardes, Phys. Rev. **120**, 1927 (1960).

³L. Goldstein, Ann. Phys. (N.Y.) **8**, 390 (1959).

⁴R. L. Mills, E. R. Grilly, and S. G. Sydorik, Ann. Phys. (N.Y.) **12**, 41 (1961).

⁵E. C. Heltemes and C. A. Swenson, Phys. Rev. **128**, 1512 (1962).

⁶E. D. Adams and G. C. Straty, to be published.

REFLECTION STUDIES OF EXCITONS IN LIQUID AND SOLID XENON*

David Beaglehole

Institute for the Study of Metals, The University of Chicago, Chicago, Illinois

(Received 23 August 1965)

In a number of insulating crystals, there exist, in addition to the well-known hydrogenic excitons lying below the threshold energies for direct interband transitions, extra excitons which lie in the continuum above the threshold. For instance, the solid-xenon absorption data taken by Baldini¹ show a strong broad line at 10.3 eV lying in the region of continuous absorption. Several models have been proposed to explain these extra excitons. Overhauser² suggested that just as the conventional excitons may be pictured in an atomic model as formed by the binding of atomic *s* electrons around the *p* hole, so might the extra excitons correspond to the binding of atomic *d* electrons. Phillips approached the problem from the band model. Here the conventional exciton is pictured as a conduction electron bound to the valence-band hole. The localized electron's wave packet is made up from conduction states near Γ in the Brillouin zone, where the high density of states allows the electron to take advantage of the potential energy of the hole with little gain of kinetic energy. Phillips³ therefore suggested that the extra excitons may arise kinematically from the binding of conduction electrons whose wave packets are formed from other regions of *k* space having high density of states—in fact, in the case of xenon, from the saddle points at *L* and *X* in the Brillouin zone. This approach appears to be successful for shallow extra excitons in semiconductors.⁴

At least from the simplest viewpoint it seems essential for the formation of this second type of exciton that the medium have long-range

order, for it is the periodic structure of the crystal which produces the high density of states at the Brillouin zone boundary. Phillips therefore suggested that a study of the exciton spectrum of liquid xenon would serve to show just how critically these states depend upon crystalline properties.

A comparison between the liquid- and solid-xenon spectra is reported here. The liquid exciton spectrum in fact is found to be very similar to that of the solid just below the melting point. The lower lying exciton states are broadened by the increased disorder, and, of special interest, the extra exciton at 10.3 eV is still present in the liquid.

Liquid-xenon's high vapor pressure makes it essential for the sample to be contained in a windowed cell. The light reflected from a lithium-fluoride window has been measured when the cell is first empty, and then filled, the back surface of the window (with a reflectivity R_b) now forming an interface between lithium fluoride and xenon. The ratio of the total light reflected from both surfaces of the window of the filled cell $R(2)$ to that reflected from the empty cell $R(1)$ may be shown to be approximately

$$\frac{R(2)}{R(1)} \cong \frac{1 + T^2 R_b(2)}{1 + T^2 R_b(1)}, \quad (1)$$

where T is the fraction of the light transmitted by the window. $R_b(2)$ may be found from Eq. (1) if the known properties of the window material⁵ are used. If $n + ik$ is the complex